Neurochemistry International 129 (2019) 104497

Contents lists available at ScienceDirect

Neurochemistry International

journal homepage: www.elsevier.com/locate/neuint

PARP inhibition *in vivo* blocks alcohol-induced brain neurodegeneration and neuroinflammatory cytosolic phospholipase A2 elevations

Dimitrios E. Kouzoukas[a,d,f,*], Jennifer A. Schreiber[b,d], Nuzhath F. Tajuddin[a], Simon Kaja[a,b,c,d,e,f], Edward J. Neafsey[a], Hee-Yong Kim[g], Michael A. Collins[a,b,d]

[a] Department of Molecular Pharmacology & Therapeutics, Loyola University Chicago, Maywood, IL, USA
[b] Neuroscience Graduate Program, Loyola University Chicago, Maywood, IL, USA
[c] Department of Ophthalmology, Loyola University Chicago, Maywood, IL, USA
[d] Alcohol Research Program, Loyola University Chicago, Maywood, IL, USA
[e] Burn Shock Trauma Research Institute, Loyola University Chicago, Maywood, IL, USA
[f] Research Service, Edward Hines Jr. VA Hospital, Hines, IL, USA
[g] Laboratory of Molecular Signaling, National Institute of Alcoholism and Alcohol Abuse, National Institutes of Health, Bethesda, MD, USA

ARTICLE INFO

Keywords:
Alcohol
Cytosolic phospholipase A2
Neurodegeneration
Poly(ADP-Ribose) polymerase
Veliparib

ABSTRACT

Chronic alcoholism promotes brain damage that impairs memory and cognition. High binge alcohol levels in adult rats also cause substantial neurodamage to memory-linked regions, notably, the hippocampus (HC) and entorhinal cortex (ECX). Concurrent with neurodegeneration, alcohol elevates poly (ADP-ribose) polymerase-1 (PARP-1) and cytosolic phospholipase A2 (cPLA2) levels. PARP-1 triggers necrosis when excessively activated, while cPLA2 liberates neuroinflammatory ω-6 arachidonic acid. Inhibitors of PARP exert *in vitro* neuroprotection while suppressing cPLA2 elevations in alcohol-treated HC-ECX slice cultures. Here, we examined *in vivo* neuroprotection and cPLA2 suppression by the PARP inhibitor, veliparib, in a recognized adult rat model of alcohol-binging. Adult male rats received Vanilla Ensure containing alcohol (ethanol, 7.1 ± 0.3 g/kg/day), or control (dextrose) ± veliparib (25 mg/kg/day), by gavage 3x daily for 4 days. Rats were sacrificed on the morning after the final binge. HC and ECX neurodegeneration was assessed in fixed sections by Fluoro-Jade B (FJB) staining. Dorsal HC, ventral HC, and ECX cPLA2 levels were quantified by immunoblotting. Like other studies using this model, alcohol binges elevated FJB staining in the HC (dentate gyrus) and ECX, indicating neurodegeneration. Veliparib co-treatment significantly reduced dentate gyrus and ECX neurodegeneration by 79% and 66%, respectively. Alcohol binges increased cPLA2 in the ventral HC by 34% and ECX by 72%, which veliparib co-treatment largely prevented. Dorsal HC cPLA2 levels remained unaffected by alcohol binges, consistent with negligible FJB staining in this brain region. These *in vivo* results support an emerging key role for PARP in binge alcohol-induced neurodegeneration and cPLA2-related neuroinflammation.

1. Introduction

A prominent outcome of chronic alcohol misuse and binge alcoholism is an elevated risk of cognitive abnormalities including dementia, and corresponding damage to supporting brain structures (Erdozain et al., 2014; Harper, 2009). Excluding instances of thiamine malnutrition or hepatic dysfunction, chronic alcohol misuse comprises ~10% of early onset dementia cases (Cheng et al., 2017). As in humans (Erdozain et al., 2014; Harper, 2009; Wilson et al., 2017), binge alcohol-related neurodamage in rodent models typically involves structures supporting learning and memory, including the hippocampus (HC) and entorhinal cortex (ECX) (Collins et al., 1996; Obernier et al., 2002; Vetreno et al., 2011). Neuroinflammation is also evident in these brain regions.

Concerning phospholipase-derived neuroinflammation, we documented that repeated alcohol binges in rats elevated levels of cytosolic phospholipase A2 (cPLA2 IVA), which is responsible for liberating the ω-6 proinflammatory fatty acid, arachidonic acid, from membrane phospholipids (Tajuddin et al., 2014). In other neuroinflammatory pathways, alcohol binging raised levels of the neuroinflammatory alarmin, high mobility group box 1 (HMGB1), and its receptors in rodent and postmortem alcoholic brains (Crews et al., 2013; Vetreno et al., 2013). Alcohol binging also elevated CD11B, an indicator of primed microglia that exacerbates neuroinflammatory responses

* Corresponding author. Research Service, Edward Hines Jr. VA Hospital, 5000 South 5th Avenue, MC-151, Hines, IL, 60141, USA.
E-mail address: dimitrios.kouzoukas@va.gov (D.E. Kouzoukas).

https://doi.org/10.1016/j.neuint.2019.104497
Received 3 May 2019; Received in revised form 17 June 2019; Accepted 25 June 2019
Available online 25 June 2019
0197-0186/ Published by Elsevier Ltd.

(Marshall et al., 2016). Collectively, these findings indicate that binge alcohol exposure drives neuroinflammatory pathways linked to neurodegeneration in vulnerable brain regions.

We previously reported that alcohol-induced neurodamage associated with elevated levels of poly (ADP-ribose) polymerase-1 (PARP-1) in adult rat HC and ECX and in organotypic HC-ECX slice cultures (Collins et al., 2014; Tajuddin et al., 2014). Although PARP is a key DNA repair enzyme, its overactivation can trigger regulated necrosis of neurons (parthanatos) (Fatokun et al., 2014). Indeed, blocking PARP activity with pharmacological inhibitors in the alcohol-binged HC-ECX slice cultures reduced or prevented neurodegeneration (Tajuddin et al., 2018). Furthermore, PARP inhibition in brain slice cultures prevented binge alcohol's augmentation of cPLA2 levels (Tajuddin et al., 2018), revealing a previously unacknowledged connection between neuronal death by brain PARP overactivation and the cPLA2 neuroinflammatory pathway.

In the current study, we tested whether the brain-penetrable PARP inhibitor, veliparib, counteracted alcohol-induced neurodegeneration and associated neuroinflammatory changes in cPLA2 in a 4-day severe binge intoxication model (Collins et al., 1996; Majchrowicz, 1975; Tajuddin et al., 2014). It differs from our previous studies (Tajuddin et al., 2013, 2014, 2018) by focusing on PARP inhibition and prevention of cPLA2 changes *in vivo*. The results indicate that PARP mediates binge alcohol-induced neurodegeneration and neuroinflammatory cPLA2 upregulation in the HC and ECX, consistent with previous *in vitro* results (Tajuddin et al., 2018).

2. Materials and methods

2.1. Alcohol exposure and pharmacological treatment

Experiments were approved by the Loyola University Chicago Institutional Animal Care and Use Committee and performed according to the guidelines of the National Institutes of Health. Adult male Sprague Dawley rats (321.0 ± 1.9 g) received alcohol (0–5 g/kg ethanol) or dextrose caloric supplement (control) in Vanilla Ensure Plus (Abbott Laboratories, Abbott Park, IL) by gavage every 8 h for 4 days (4–7 rats/group) (Collins et al., 1996; Faingold, 2008; Majchrowicz, 1975). After a 5 g/kg alcohol priming dose, subsequent alcohol treatments were titrated according to a 6-point scale based on a visual inspection of intoxication behaviors: 0 = normal movement (5 g/kg), 1 = hypoactive (4 g/kg), 2 = ataxia (3 g/kg), 3 = delayed righting reflex, ataxia with no abdominal elevation (2 g/kg), 4 = loss of righting reflex (1 g/kg), and 5 = loss of eye blink reflex (0 g/kg) (Faingold, 2008; Nixon and Crews, 2004). This scale highly correlates with blood alcohol concentrations (BAC). Rats received the PARP inhibitor, veliparib (ApexBio, Boston, MA; 25 mg/kg/day) orally in control or alcohol solutions. This dose was chosen because it provided a maximal effect, while being well tolerated (Donawho et al., 2007). Veliparib was chosen due to its high oral bioavailability, long half-life, and efficiency in penetrating the blood-brain-barrier (Donawho et al., 2007; Li et al., 2011; Muscal et al., 2010). Using a commercial kit (Pointe Scientific, Canton, MI), peak BACs were measured in serum of tail blood collected 90 min after the 1st gavage on day 4.

2.2. Tissue collection & sectioning

On the morning after the final gavage, isoflurane-anesthetized rats were transcardially perfused with ice-cold phosphate-buffered saline (PBS). Brains were removed, split along the midsagittal plane, and frozen in isopentane cooled by a methanol/dry ice slurry. Horizontal sections (25 μm) from one hemisphere, taken every 0.5 mm from −8.6 to −5.6 mm below bregma, were thaw-mounted onto positively-charged glass slides (Diamond; Globe Scientific, Paramus, NJ). From the other hemisphere, HC and ECX were microdissected on ice (Chiu et al., 2007). Isolated HC were bisected into dorsal and ventral regions. All samples were stored at −80 °C.

2.3. Fluoro-Jade B staining for neurodegeneration and analysis

Fluoro-Jade B (FJB) is a well-accepted fluorescent marker of dead or dying neurons, including in this alcohol binge model (Leasure and Nixon, 2010; Obernier et al., 2002). Sections were fixed (4% paraformaldehyde in PBS, 15 min), air-dried, then processed for FJB (EMD Millipore, Billerica, MA) staining as described (Leasure and Nixon, 2010; Obernier et al., 2002). Slides were immersed in solutions of 1% sodium hydroxide in 80% ethanol for 5 min, 70% ethanol for 2 min, distilled water for 2 min, 0.06% potassium permanganate for 10 min, distilled water for 2 min, 0.01% FJB in 0.1% acetic acid for 20 min, and washed 3x with distilled water for 1 min. Air-dried sections were sealed under coverglass with Cytoseal 50 (Richard-Allan Scientific, San Diego, CA) and dried overnight.

Sections were imaged using a Cytation5 digital imager (BioTek, Winooski, VT). Structures were determined by a stereotaxic atlas (Paxinos and Watson, 2014). HC and ECX regions of interest (ROIs) were drawn on section scans using ImageJ (NIH, Bethesda, MD), and areas (mm^2) measured. In the dentate gyrus (DG), FJB+ cells mostly appeared in the granule cell layer, whereas ECX FJB+ cells localized to layer III (Fig. 1A) similar to previous reports (Collins et al., 1996; Obernier et al., 2002). ROIs were created for entire structures. Since ROI area, and consequently FJB+ cell counts, depended on dorsal-ventral brain coordinates, counts were normalized to the ROI surface area and averaged across sections for each rat. Only FJB+ cells that resembled neuronal soma morphologically (see insets, Fig. 1A) were counted in ROIs. Counts were verified by a blinded observer. For each rat, a minimum of three horizontal sections (an average of 5.40 ± 0.22 and 5.50 ± 0.25 sections for each DG and LEnt, respectively) were analyzed.

2.4. Western blotting

Dorsal HC, ventral HC, and ECX were homogenized in cold lysis buffer (1 mg tissue/12 μl RIPA buffer; Sigma, Burlington, MA) containing protease and phosphatase inhibitor cocktail (50X, Sigma, Burlington, MA), gently shaken for 2 h (4 °C), and then centrifuged to pellet debris. Collected supernatants were aliquoted and frozen at −80 °C. Bicinchoninic acid assay (Pierce Biotech, Rockford, IL) determined total proteins concentrations. Reduced samples (40 g protein +100 μM dithiothreitol) in Laemmli buffer (Bio-Rad, Hercules, CA), were separated by SDS-PAGE in 4–20% gradient Bis-Tris gels (Genscript, Piscataway, NJ) and transferred to nitrocellulose membranes (Bio-Rad, Hercules, CA). Cytosolic PLA2 was quantified using a primary antibody (sc-454 at 1:250 dilution; Santa Cruz Biotech, Dallas, TX), a horseradish peroxidase-linked secondary antibody (sc-516102; Santa Cruz Biotech, Dallas, TX), and the SuperSignal West Femto Substrate ECL kit (ThermoFisher Scientific, Waltham, MA). The loading control, GAPDH (probed with sc-365062; Santa Cruz Biotech, Dallas, TX), was measured after stripping (Restore; Thermo Fisher Scientific, Waltham, MA). All blot images were acquired by a Chemidoc XRS imaging system (BioRad, Hercules, CA) and analyzed in ImageJ (NIH, Bethesda, MD) using rolling ball background subtraction. Relative density values were calculated as the target protein band density divided by that of GAPDH, then expressed as a percent of control group levels (mean ± SEM) in each blot. Samples run on multiple blots were normalized to their respective blot's control group, then averaged.

2.5. Statistical analyses

ANOVAs determined significant interactions between factors and differences between treatment groups. As low numbers in some groups (4 rats) may affect ANOVA interpretation, Kruskal-Wallis Tests were also performed. In all cases, these agreed with the results of the

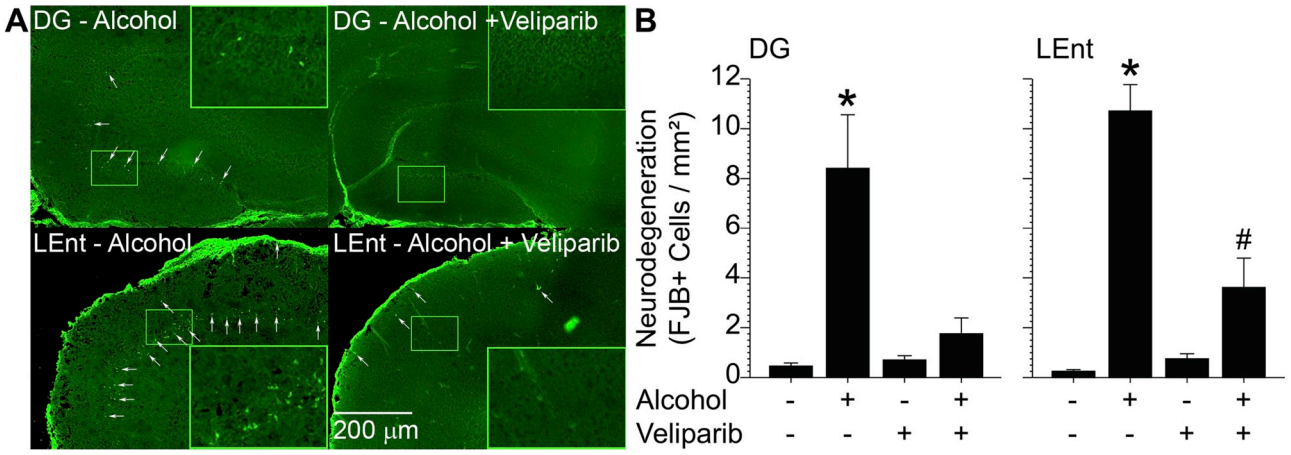

Fig. 1. PARP inhibitor, veliparib, reduced alcohol-related neurodegeneration in dentate gyrus (DG) and lateral entorhinal cortex (LEnt). A) Panels show neurodegeneration (FJB labeling) in rat dentate gyrus (DG; above) and lateral entorhinal cortex (LEnt; below) after 4 days of alcohol binges. White arrows identify examples of FJB+ (degenerating) cells. For each viewfield, insets are the boxed areas magnified 300%. ROIs were drawn on horizontal HC and ECX scans using ImageJ (NIH, Bethesda, MD) and areas (mm^2) measured. For each ROI, FJB+ cells were counted and then verified by a blinded observer. B) Bar graphs show that veliparib (25 mg/kg/day) reduced alcohol-induced DG and LEnt neurodegeneration by 79.1% and 66.3%, respectively. N = 4–5 rats/group. (* different from all, # different from alcohol and no treatment control groups; Tukey's HSD, $p \leq 0.05$).

ANOVAs. Post-hoc analyses consisted of Tukey's Honest Significant Difference (HSD) test, or planned comparisons (Student's t-tests) where indicated. For Western blot data, statistical extreme outliers, defined as greater than 3.0 × interquartile range, were removed (one data point). Outliers in the control group (no alcohol or veliparib) were kept, since all values were normalized (100%) to the cPLA2 levels in the control group within each blot.

All data are presented as mean ± SEM, with statistical differences of $p \leq 0.05$ considered significant. All statistical analyses were performed using SPSS Statistics (IBM, New York, NY). Supplemental Table 1 provides a summary of all omnibus tests described under the Results section.

3. Results

Weight loss is typical and expected with this binge alcohol intoxication model (Marshall et al., 2016). Significant weight loss (Tukey's HSD, $p \leq 0.05$) over the 4-day binge paradigm occurred in animals receiving either Alcohol (14.5 ± 0.7%) or Alcohol + Veliparib (9.3 ± 2.5%) (Table 1). No differences in peak BAC (Student's t-test, $p > 0.05$) were detected in alcohol-binged rats given veliparib (25 mg/kg/day) or not (369.5 ± 36.0 vs. 350.6 ± 31.1 mg/dl, Table 1). Veliparib-treated rats appeared slightly less intoxicated as determined by the 6-point visual intoxication scale (1.8 ± 0.3 vs. 2.4 ± 0.1; Student's t-test, $p \leq 0.05$). This difference necessitated that rats treated with alcohol and veliparib receive more alcohol overall than rats receiving only alcohol (9.0 ± 0.7 vs. 7.1 ± 0.3 g/kg/day; Student's t-test, $p \leq 0.05$).

3.1. Veliparib reduced binge alcohol neurodegeneration in dentate gyrus (DG) and lateral ECX (LEnt)

To examine alcohol-induced neurodegeneration, ROIs for HC and ECX were drawn on section images and FJB+ cells were counted. As shown in Table 2, control rat sections showed few FJB+ cells (< 0.75 cells/mm^2) in the HC and ECX, and veliparib alone did not raise FJB+ cell counts (Tukey's HSD, $p > 0.05$ vs. control) in any examined brain region. Binge alcohol treatment promoted significant DG and LEnt neurodegeneration (Table 2 and Fig. 1; Tukey's HSD, $p \leq 0.05$) as shown by elevated counts of FJB+ cells *vs.* control in the DG (8.4 ± 2.1 cells/mm^2) and LEnt (10.7 ± 1.1 cells/mm^2). No significant changes in FJB+ cell counts were seen in other HC regions (cornu ammonis and subiculum) or in the medial entorhinal cortex, agreeing with earlier cupric-silver neurodegeneration stain results (Collins et al., 1996). No FJB+ cells appeared in the dorsal HC (above bregma −4.6 mm). Two-way ANOVAs (2 × 2) revealed the interaction of veliparib and alcohol exposure on FJB+ counts in the DG and LEnt ($p \leq 0.05$, Fig. 1B). Co-treatment with veliparib in alcohol-binged rats promoted significant neuroprotection as evidenced by a 78.6% reduction in FJB+ cell counts (1.8 ± 0.6 cells/mm^2) in DG, and a 66.4% reduction in FJB+ counts (3.6 ± 1.2 cells/mm^2) in LEnt (Tukey's HSD, $p \leq 0.05$ vs alcohol only; Table 2 and Fig. 1).

3.2. Veliparib blocked the binge alcohol-induced increase of cPLA2 levels in ventral HC and ECX

Since veliparib diminished neurodegeneration (FJB+ cells) in the ventral HC and LEnt (Table 2), we evaluated whether PARP inhibition also affected neuroinflammatory changes in cPLA2 in these regions.

Table 1
Weight and alcohol intake across treatment groups.

Group	N	Initial Weight (g)	Final Weight (g)	Weight Loss (%)	Alcohol Intake (g/kg/day)	Peak BAC (mg/dl)
Control	5	320 ± 4.8	320 ± 4.0	0.2 ± 1.1	–	–
Control + Veliparib	5	322 ± 1.9	327 ± 3.7	−1.3 ± 0.6	–	–
Alcohol	5	321 ± 5.0	274 ± 5.6 *	14.5 ± 0.7 *	7.1 ± 0.3	359.0 ± 31.8
Alcohol + Veliparib	4	320 ± 3.7	290 ± 9.6 *	9.3 ± 2.6 *	9.0 ± 0.7 #	378.4 ± 36.9

Means ± SEM are displayed. (* different from control groups, Tukey's HSD; # different from alcohol alone, Student's t-test, $p \leq 0.05$). Peak BAC in alcohol-treated groups averaged 79.8 ± 4.9 mM (367.7 ± 22.6 mg/dl). Rats in the control groups received no alcohol.

Table 2
The effect of veliparib on alcohol-induced neurodegeneration in the HC and ECX.

Group	N	Coor. (mm)	Neurodegeneration (FJB+ Cells/ mm^2)						
			Hippocampus					Entorhinal Cortex	
			S	CA1	CA2	CA3	DG	MEnt	LEnt
Control	5	-6.96 ± 0.05	0.5 ± 0.2	0.1 ± 0.1	0.5 ± 0.2	0.2 ± 0.1	0.5 ± 0.1	0.7 ± 0.1	0.3 ± 0.1
Control + Veliparib	5	-7.00 ± 0.03	0.2 ± 0.1	0.3 ± 0.1	0.2 ± 0.1	0.5 ± 0.1	0.7 ± 0.2	1.1 ± 0.6	0.8 ± 0.2
Alcohol	5	-7.07 ± 0.14	1.0 ± 0.4	0.6 ± 0.2	0.9 ± 0.3	1.6 ± 0.6	8.4 ± 2.1*	2.1 ± 0.4	10.7 ± 1.1*
Alcohol + Veliparib	4	-7.15 ± 0.03	0.5 ± 0.2	0.6 ± 0.4	0.5 ± 0.2	0.7 ± 0.2	1.8 ± 0.6	1.6 ± 0.4	3.6 ± 1.2

Degenerating neurons (FJB+ Cells) and ROI areas (mm^2) were determined in the HC and ECX sections of rats receiving treatments. Means ± SEM are displayed. Four days of alcohol binges caused neurodegeneration in the dentate gyrus (DG) and lateral entorhinal cortex (LEnt) (* different from all, Tukey's HSD, $p \leq 0.05$), which was prevented by the PARP inhibitor, veliparib (25 mg/kg/day). Other abbreviations: Vertical coordinates (Coor.); Cornu Ammonis (CA); Medial entorhinal cortex (MEnt); Subiculum (S).

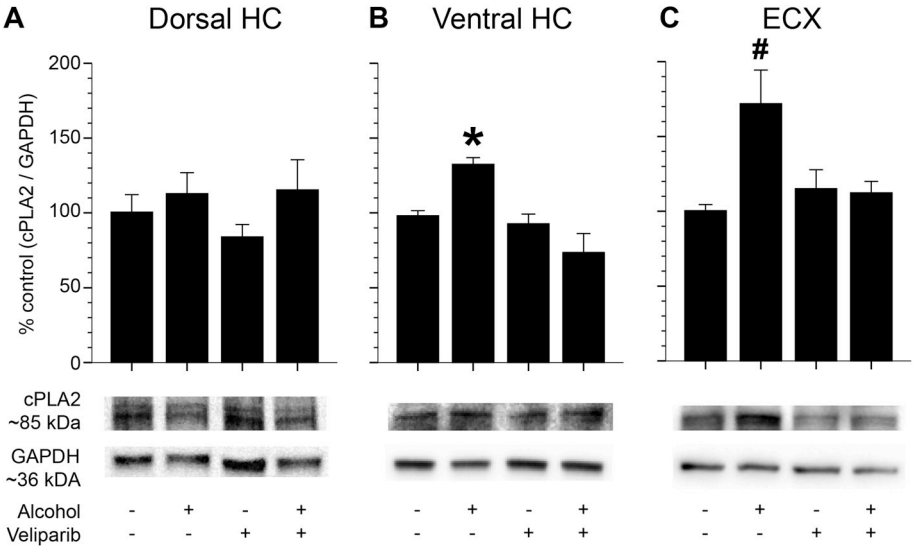

Fig. 2. PARP inhibitor, veliparib, reduced alcohol-related changes in cPLA2 levels in the HC and ECX. Representative bands from each immunoblot are shown below graphs in each panel. Band and x axis labels are at the bottom. Graphs respectively show cPLA2 levels in the dorsal HC (A), ventral HC (B), and ECX (C) normalized to GAPDH, relative to corresponding levels in controls (rats with no exposure to alcohol or veliparib). Bar graphs show that alcohol binges elevated cPLA2 levels in the ventral HC and ECX, but not in the dorsal HC. Two-way ANOVAs indicated veliparib (25 mg/kg/day) reduced alcohol-related changes in cPLA2 in the ventral HC and the ECX ($p \leq 0.05$). N = 4–7 rats/group. Differences by Tukey's HSD (one-way ANOVA) are indicated: * (different from all, $p \leq 0.05$), # (different from no treatment control group, $p \leq 0.05$).

Consistent with previous reports (Tajuddin et al., 2013, 2014), binge alcohol treatment significantly elevated cPLA2 in the ventral HC (+34.4 ± 4.4%; Tukey's HSD, $p \leq 0.05$, Fig. 2B) and in the ECX (+71.9 ± 2.3%; Tukey's HSD, $p \leq 0.05$, Fig. 2C). No cPLA2 changes from binge alcohol treatment were observed in the dorsal HC (Fig. 2A), which is consistent with FJB+ cells absent in the dorsal HC (above bregma −4.6 mm). Two-way ANOVAs (2 × 2) revealed the interaction of veliparib and alcohol exposure on cPLA2 levels in the ventral HC and ECX ($p \leq 0.05$, Fig. 2B and C). PARP inhibition by veliparib co-treatment in alcohol-binged rats abolished the amplification of cPLA2 levels in the ventral HC, suppressing cPLA2 by 44.7%. A similar reduction in cPLA2 levels (34.6%) was observed in the ECX.

4. Discussion

These results indicate that PARP overactivation plays a key role in binge alcohol-induced neurodegeneration and phospholipid-associated neuroinflammation *in vivo*. This conclusion is supported by demonstrating the *in vivo* efficacy of a PARP inhibitor in preventing alcohol neurodegeneration in vulnerable brain regions and neuroinflammatory changes in cPLA2 levels. Furthermore, this study strengthens the link between PARP and changes in phospholipid-mediated neuroinflammatory signaling by being the first *in vivo* study that links PARP activity to brain cPLA2 elevations.

The current study confirmed previous findings from alcohol-binged adult rats. Specifically, binge alcohol treatment caused HC and ECX neurodegeneration (Collins et al., 1996; Kelso et al., 2011; Obernier et al., 2002), which resembles corticolimbic patterns of brain damage in chronic alcoholics (Erdozain et al., 2014; Harper, 2009; Wilson et al., 2017). Our levels of FJB+ cells are comparable with those seen in other studies (Cippitelli et al., 2017; Kelso et al., 2011; Obernier et al., 2002). Although the current study used FJB, an often-used marker of degenerating neurons, it can also stain glial cells (Damjanac et al., 2007). Special care was taken to count cells that morphologically resembled neuronal soma. Previous studies (Collins et al., 1996; Obernier et al., 2002), using another marker of degenerating neurons, the amino cupric silver technique, in this same alcohol binge model, also incurred extensive staining in the HC and ECX structures indicating specific neurodegeneration.

Moreover, PARP inhibitor treatment (veliparib) prevented this damage *in vivo*. The current study extends earlier *in vitro* findings, which demonstrated 1) that alcohol increases enzymatic PARP activity in mouse cortical neuronal cultures (Gavin et al., 2016) and 2) that PARP inhibition protects against alcohol's neurodamage in HC-ECX slice cultures (Tajuddin et al., 2018). The current study also complements our observations of elevated PARP-1 levels in highly vulnerable brain regions (HC and ECX) of moderately binged adult rats (~3 g/kg/d alcohol) (Tajuddin et al., 2013). Although the brain expresses multiple PARP isoforms, PARP-1 is responsible for approximately 90% of the total cellular PARylation activity after DNA damage (Horvath et al., 2011). Our findings are consistent with a growing literature indicating that DNA strand breaks after pro-oxidative brain insults (i.e., stroke or trauma) may overactivate PARP-1, with its poly (ADP-ribose) products eliciting neuroinflammation and neurodegeneration (Narne et al.,

2017). They also agree with recent studies indicating alcohol binges elicit DNA damage (Moon et al., 2014; Suman et al., 2016).

Our prior studies demonstrate that binge alcohol treatment alter levels of PLA2 isoenzymes (Tajuddin et al., 2014, 2018), which can lead to neuroinflammation (Ong et al., 2010). Cytosolic PLA2 acts on membrane phospholipids to mobilize arachidonic acid, which is subsequently converted by cyclooxygenases and lipoxygenases into potent pro-inflammatory mediators—e.g., prostaglandins and leukotrienes (Calder, 2006). These products and pathways can promote formation of reactive oxygen species that contribute to neurodegeneration (Ong et al., 2010).

In previous studies (Tajuddin et al., 2013, 2014, 2018), alcohol elevated levels of secretory PLA2 (sPLA2) and total and phosphorylated (activated) cPLA2 in the HC and ECX of adult rats and brain slice cultures. Concurring with these PLA2 elevations, alcohol stimulated arachidonic acid release from brain slice cultures, while treatment with PLA2 inhibitors reduced binge alcohol-provoked neurodegeneration (Brown et al., 2009; Tajuddin et al., 2018). These data provide support for binge alcohol treatment promoting the neuroinflammatory cPLA2 pathway to facilitate neurodegeneration. It should be noted that ω-3 docosahexaenoic acid treatment also conferred neuroprotection while preventing alcohol-induced elevations in cPLA2 levels (Tajuddin et al., 2014). Together, these studies indicate that alcohol neurodegeneration relies on a cPLA2-dependent pathway.

Furthermore, alcohol-induced neuroinflammatory changes in PLA2 enzymes coincided with increased PARP levels in this laboratory's past studies (Tajuddin et al., 2014, 2018). Indeed, treatments with several PARP inhibitors normalized cPLA2 and sPLA2 levels while preventing alcohol-induced neurodegeneration in brain slice cultures (Tajuddin et al., 2018). This indicates alcohol's effect on PARP is upstream of changes in PLA2. Veliparib co-treatment in the current *in vivo* study completely normalized alcohol-induced increases in cPLA2. Collectively, these factors indicate that alcohol potentiates PLA2-mediated neuroinflammation through a mechanism involving PARP, which then leads to neurodegeneration in vulnerable brain regions.

Whether PARP upregulates cPLA2 directly by transcriptional regulation through its PAR products (Gupte et al., 2017) or indirectly is unknown. One possible indirect pathway relies on HMGB1 because cPLA2 activity and arachidonic acid elevations have been linked to toll-like receptor 4 (TLR4) activation and proinflammatory cytokines (Ruiperez et al., 2009). Indeed, reports in rats, mice, humans, and in microglial cultures (Crews et al., 2013; Marshall et al., 2016; Vetreno et al., 2013) show alcohol elevates brain HMGB1 and TLR4 levels. Supporting this conjecture, PARP inhibitors block HMGB1 elevations in alcohol-treated brain slice cultures (Tajuddin et al., 2018).

5. Conclusions

In conclusion, PARP inhibition by veliparib treatment prevented binge alcohol-induced neurodegeneration in the ventral HC and ECX, linking PARP activity to the mechanisms of binge alcohol-dependent brain neuroinjury. Alcohol binges elevated cPLA2 levels in the ventral HC and ECX, but not in the dorsal HC which lacked neurodamage. PARP inhibition also reduced related changes in levels of cPLA2 in the ventral HC and ECX. These *in vivo* results link PARP to neuroinflammatory cPLA2 activity in the mechanisms of alcohol-induced neurodegeneration. Given this connection, pharmacological inhibition of PARP might eventually be a valid neuroprotective strategy during the detoxification of chronic alcoholics, but much research remains. Future studies aimed at exploring this relationship may provide new insights into the mechanisms of alcohol-related brain damage and possible therapeutic interventions.

Conflicts of interest

Stock/equity ownership: SK (Experimentica, Ltd.); SK (K&P Scientific, LLC); Consulting: SK (Experimentica, Ltd.). SK also conducts academic research in areas similar to the business interests of Experimentica, Ltd and K&P Scientific, LLC. This arrangement's terms have been approved by Loyola University Chicago in accordance with its conflict of interest policy. This study has no other conflicts of interest.

Funding

Supported by the National Institutes of Health [U01-AA018279 to MAC, T32-AA013527 to Alcohol Research Program]. Additional support from the Dr. John P. and Therese E. Mulcahy Endowed Professorship in Ophthalmology (to SK) and United States Department of Veterans Affairs [I21-RX003170 to DEK] are gratefully acknowledged.

Acknowledgements

Dr. Kimberly Nixon in the Division of Pharmacology & Toxicology, University of Texas at Austin, generously provided technical training for FJB staining and the alcohol binge model. Dr. Vidhya Rao and Mr. Jack Kwan are recognized for providing technical assistance. Dr. Gwendolyn Kartje of the Edward Hines Jr. VA Hospital and Loyola University Chicago gave an invaluable informal review.

This work resulted from resources and facilities at Loyola University Chicago and the Edward Hines Jr. VA Hospital. The views expressed in this article are those of the authors and not necessarily that of the National Institutes of Health, the United States Department of Veterans Affairs, or the United States government.

Appendix A. Supplementary data

Supplementary data to this article can be found online at https://doi.org/10.1016/j.neuint.2019.104497.

References

Brown 3rd, J., Achille, N., Neafsey, E.J., Collins, M.A., 2009. Binge ethanol-induced neurodegeneration in rat organotypic brain slice cultures: effects of PLA2 inhibitor mepacrine and docosahexaenoic acid (DHA). Neurochem. Res. 34, 260–267.

Calder, P.C., 2006. Polyunsaturated fatty acids and inflammation. Prostagl. Leukot. Essent. Fat. Acids 75, 197–202.

Cheng, C., Huang, C.L., Tsai, C.J., Chou, P.H., Lin, C.C., Chang, C.K., 2017. Alcohol-related dementia: a systemic review of epidemiological studies. Psychosomatics 58, 331–342.

Chiu, K., Lau, W.M., Lau, H.T., So, K.F., Chang, R.C., 2007. Micro-dissection of rat brain for RNA or protein extraction from specific brain region. J. Vis. Exp. 269.

Cippitelli, A., Domi, E., Ubaldi, M., Douglas, J.C., Li, H.W., Demopulos, G., Gaitanaris, G., Roberto, M., Drew, P.D., Kane, C.J.M., Ciccocioppo, R., 2017. Protection against alcohol-induced neuronal and cognitive damage by the PPARgamma receptor agonist pioglitazone. Brain Behav. Immun. 64, 320–329.

Collins, M.A., Corso, T.D., Neafsey, E.J., 1996. Neuronal degeneration in rat cerebrocortical and olfactory regions during subchronic "binge" intoxication with ethanol: possible explanation for olfactory deficits in alcoholics. Alcohol Clin. Exp. Res. 20, 284–292.

Collins, M.A., Tajuddin, N., Moon, K.H., Kim, H.Y., Nixon, K., Neafsey, E.J., 2014. Alcohol, phospholipase A2-associated neuroinflammation, and omega3 docosahexaenoic acid protection. Mol. Neurobiol. 50, 239–245.

Crews, F.T., Qin, L., Sheedy, D., Vetreno, R.P., Zou, J., 2013. High mobility group box 1/Toll-like receptor danger signaling increases brain neuroimmune activation in alcohol dependence. Biol. Psychiatry 73, 602–612.

Damjanac, M., Rioux Bilan, A., Barrier, L., Pontcharraud, R., Anne, C., Hugon, J., Page, G., 2007. Fluoro-Jade B staining as useful tool to identify activated microglia and astrocytes in a mouse transgenic model of Alzheimer's disease. Brain Res. 1128, 40–49.

Donawho, C.K., Luo, Y., Luo, Y., Penning, T.D., Bauch, J.L., Bouska, J.J., Bontcheva-Diaz, V.D., Cox, B.F., DeWeese, T.L., Dillehay, L.E., Ferguson, D.C., Ghoreishi-Haack, N.S., Grimm, D.R., Guan, R., Han, E.K., Holley-Shanks, R.R., Hristov, B., Idler, K.B., Jarvis, K., Johnson, E.F., Kleinberg, L.R., Klinghofer, V., Lasko, L.M., Liu, X., Marsh, K.C., McGonigal, T.P., Meulbroek, J.A., Olson, A.M., Palma, J.P., Rodriguez, L.E., Shi, Y., Stavropoulos, J.A., Tsurutani, A.C., Zhu, G.D., Rosenberg, S.H., Giranda, V.L., Frost, D.J., 2007. ABT-888, an orally active poly(ADP-ribose) polymerase inhibitor that potentiates DNA-damaging agents in preclinical tumor models. Clin. Cancer Res. 13, 2728–2737.

Erdozain, A.M., Morentin, B., Bedford, L., King, E., Tooth, D., Brewer, C., Wayne, D.,

Johnson, L., Gerdes, H.K., Wigmore, P., Callado, L.F., Carter, W.G., 2014. Alcohol-related brain damage in humans. PLoS One 9, e93586.
Faingold, C.L., 2008. The Majchrowicz binge alcohol protocol: an intubation technique to study alcohol dependence in rats. Curr. Protoc. Neurosci. 9 Unit 9 28.
Fatokun, A.A., Dawson, V.L., Dawson, T.M., 2014. Parthanatos: mitochondrial-linked mechanisms and therapeutic opportunities. Br. J. Pharmacol. 171, 2000–2016.
Gavin, D.P., Kusumo, H., Sharma, R.P., Guizzetti, M., 2016. Ethanol-induced changes in poly (ADP ribose) polymerase and neuronal developmental gene expression. Neuropharmacology 110, 287–296.
Gupte, R., Liu, Z., Kraus, W.L., 2017. PARPs and ADP-ribosylation: recent advances linking molecular functions to biological outcomes. Genes Dev. 31, 101–126.
Harper, C., 2009. The neuropathology of alcohol-related brain damage. Alcohol Alcohol 44, 136–140.
Horvath, E.M., Zsengeller, Z.K., Szabo, C., 2011. Quantification of PARP activity in human tissues: ex vivo assays in blood cells and immunohistochemistry in human biopsies. Methods Mol. Biol. 780, 267–275.
Kelso, M.L., Liput, D.J., Eaves, D.W., Nixon, K., 2011. Upregulated vimentin suggests new areas of neurodegeneration in a model of an alcohol use disorder. Neuroscience 197, 381–393.
Leasure, J.L., Nixon, K., 2010. Exercise neuroprotection in a rat model of binge alcohol consumption. Alcohol Clin. Exp. Res. 34, 404–414.
Li, X., Delzer, J., Voorman, R., de Morais, S.M., Lao, Y., 2011. Disposition and drug-drug interaction potential of veliparib (ABT-888), a novel and potent inhibitor of poly (ADP-ribose) polymerase. Drug Metab. Dispos. 39, 1161–1169.
Majchrowicz, E., 1975. Induction of physical dependence upon ethanol and the associated behavioral changes in rats. Psychopharmacologia 43, 245–254.
Marshall, S.A., Geil, C.R., Nixon, K., 2016. Prior binge ethanol exposure potentiates the microglial response in a model of alcohol-induced neurodegeneration. Brain Sci. 6.
Moon, K.H., Tajuddin, N., Brown 3rd, J., Neafsey, E.J., Kim, H.Y., Collins, M.A., 2014. Phospholipase A2, oxidative stress, and neurodegeneration in binge ethanol-treated organotypic slice cultures of developing rat brain. Alcohol Clin. Exp. Res. 38, 161–169.
Muscal, J.A., Thompson, P.A., Giranda, V.L., Dayton, B.D., Bauch, J., Horton, T., McGuffey, L., Nuchtern, J.G., Dauser, R.C., Gibson, B.W., Blaney, S.M., Su, J.M., 2010. Plasma and cerebrospinal fluid pharmacokinetics of ABT-888 after oral administration in non-human primates. Cancer Chemother. Pharmacol. 65, 419–425.
Narne, P., Pandey, V., Simhadri, P.K., Phanithi, P.B., 2017. Poly(ADP-ribose)polymerase-1 hyperactivation in neurodegenerative diseases: the death knell tolls for neurons. Semin. Cell Dev. Biol. 63, 154–166.
Nixon, K., Crews, F.T., 2004. Temporally specific burst in cell proliferation increases hippocampal neurogenesis in protracted abstinence from alcohol. J. Neurosci. 24, 9714–9722.
Obernier, J.A., Bouldin, T.W., Crews, F.T., 2002. Binge ethanol exposure in adult rats causes necrotic cell death. Alcohol Clin. Exp. Res. 26, 547–557.
Ong, W.Y., Farooqui, T., Farooqui, A.A., 2010. Involvement of cytosolic phospholipase A(2), calcium independent phospholipase A(2) and plasmalogen selective phospholipase A(2) in neurodegenerative and neuropsychiatric conditions. Curr. Med. Chem. 17, 2746–2763.
Paxinos, G., Watson, C., 2014. Paxino's and Watson's the Rat Brain in Stereotaxic Coordinates, seventh ed. Elsevier/AP, Academic Press is an imprint of Elsevier, Amsterdam ; Boston.
Ruiperez, V., Astudillo, A.M., Balboa, M.A., Balsinde, J., 2009. Coordinate regulation of TLR-mediated arachidonic acid mobilization in macrophages by group IVA and group V phospholipase A2s. J. Immunol. 182, 3877–3883.
Suman, S., Kumar, S., N'Gouemo, P., Datta, K., 2016. Increased DNA double-strand break was associated with downregulation of repair and upregulation of apoptotic factors in rat hippocampus after alcohol exposure. Alcohol 54, 45–50.
Tajuddin, N., Kim, H.Y., Collins, M.A., 2018. PARP inhibition prevents ethanol-induced neuroinflammatory signaling and neurodegeneration in rat adult-age brain slice cultures. J. Pharmacol. Exp. Ther. 365, 117–126.
Tajuddin, N., Moon, K.H., Marshall, S.A., Nixon, K., Neafsey, E.J., Kim, H.Y., Collins, M.A., 2014. Neuroinflammation and neurodegeneration in adult rat brain from binge ethanol exposure: abrogation by docosahexaenoic acid. PLoS One 9, e101223.
Tajuddin, N.F., Przybycien-Szymanska, M.M., Pak, T.R., Neafsey, E.J., Collins, M.A., 2013. Effect of repetitive daily ethanol intoxication on adult rat brain: significant changes in phospholipase A2 enzyme levels in association with increased PARP-1 indicate neuroinflammatory pathway activation. Alcohol 47, 39–45.
Vetreno, R.P., Hall, J.M., Savage, L.M., 2011. Alcohol-related amnesia and dementia: animal models have revealed the contributions of different etiological factors on neuropathology, neurochemical dysfunction and cognitive impairment. Neurobiol. Learn. Mem. 96, 596–608.
Vetreno, R.P., Qin, L., Crews, F.T., 2013. Increased receptor for advanced glycation end product expression in the human alcoholic prefrontal cortex is linked to adolescent drinking. Neurobiol. Dis. 59, 52–62.
Wilson, S., Bair, J.L., Thomas, K.M., Iacono, W.G., 2017. Problematic alcohol use and reduced hippocampal volume: a meta-analytic review. Psychol. Med. 47, 2288–2301.